Biochemical Journal (2016) **473** 3997–4009
DOI: 10.1042/BCJ20160696

PORTLAND PRESS

Research Article

The HemQ coprohaem decarboxylase generates reactive oxygen species: implications for the evolution of classical haem biosynthesis

Charlie Hobbs[1], Harry A. Dailey[2,3,4] and Mark Shepherd[1]

[1]School of Biosciences, University of Kent, Canterbury, Kent CT2 7NJ, U.K.; [2]Biomedical and Health Sciences Institute, University of Georgia, Athens, GA 30602, U.S.A.; [3]Department of Microbiology, University of Georgia, Athens, GA 30602, U.S.A.; and [4]Department of Biochemistry and Molecular Biology, University of Georgia, Athens, GA 30602, U.S.A.

Correspondence: Mark Shepherd (m.shepherd@kent.ac.uk)

OPEN ACCESS

Bacteria require a haem biosynthetic pathway for the assembly of a variety of protein complexes, including cytochromes, peroxidases, globins, and catalase. Haem is synthesised via a series of tetrapyrrole intermediates, including non-metallated porphyrins, such as protoporphyrin IX, which is well known to generate reactive oxygen species in the presence of light and oxygen. *Staphylococcus aureus* has an ancient haem biosynthetic pathway that proceeds via the formation of coproporphyrin III, a less reactive porphyrin. Here, we demonstrate, for the first time, that HemY of *S. aureus* is able to generate both protoporphyrin IX and coproporphyrin III, and that the terminal enzyme of this pathway, HemQ, can stimulate the generation of protoporphyrin IX (but not coproporphyrin III). Assays with hydrogen peroxide, horseradish peroxidase, superoxide dismutase, and catalase confirm that this stimulatory effect is mediated by superoxide. Structural modelling reveals that HemQ enzymes do not possess the structural attributes that are common to peroxidases that form compound I [Fe^{IV}═O]$^{+}$, which taken together with the superoxide data leaves Fenton chemistry as a likely route for the superoxide-mediated stimulation of protoporphyrinogen IX oxidase activity of HemY. This generation of toxic free radicals could explain why HemQ enzymes have not been identified in organisms that synthesise haem via the classical protoporphyrin IX pathway. This work has implications for the divergent evolution of haem biosynthesis in ancestral microorganisms, and provides new structural and mechanistic insights into a recently discovered oxidative decarboxylase reaction.

Introduction

Haem is an important cofactor required for a variety of functions, including the transport of oxygen and carbon dioxide in multicellular organisms, cytochrome-mediated electron transfer in respiratory chains, and detoxification of nitric oxide by bacterial globin proteins. In addition, peroxidases, catalases, and cytochrome P450s also utilise haem as a cofactor. Until recently, it was generally accepted that the terminal stages of haem synthesis were catalysed by four enzymatic steps via a pathway from uroporphyrinogen III ending in the insertion of ferrous iron. In the so-called classical pathway, uroporphyrinogen III undergoes decarboxylation to form coproporphyrinogen, whereby acetyl side chains are converted into methyl groups with concomitant release of CO_2. Coproporphyrinogen III is then converted into protoporphyrinogen IX via an oxidative decarboxylation reaction that removes carboxy groups from the propionates on rings A and B leaving vinyl substituents. There are two alternative enzymes that can catalyse this process, HemF and HemN. The reaction involving HemF is oxygen-dependent, with molecular oxygen being used as the final electron acceptor. This form of coproporphyrinogen oxidase is mainly found in eukaryotic organisms, whereas the HemN enzyme

Received: 20 July 2016
Revised: 1 September 2016
Accepted: 5 September 2016

Accepted Manuscript online: 5 September 2016
Version of Record published: 27 October 2016

Biochemical Journal (2016) **473** 3997–4009
DOI: 10.1042/BCJ20160696

that is found in many Gram-negative bacteria is oxygen-independent [1]. The penultimate step in the synthesis of haem via this pathway is the six-electron oxidation of protoporphyrinogen IX to protoporphyrin IX by protoporphyrinogen IX oxidase (also known as PPO). As with the coproporphyrinogen oxidase reaction, there are oxygen-dependent and oxygen-independent PPO enzymes. The oxygen-dependent reaction, which is catalysed by the HemY enzyme, uses oxygen for the terminal electron acceptor, whereas the oxygen-independent HemG and HemJ enzymes shuttle the electrons into the respiratory chain [2–4]. Finally, a ferrous iron is inserted into protoporphyrin IX by the terminal enzyme of the pathway, ferrochelatase.

An alternative pathway for haem biosynthesis was discovered recently that produces haem via a sirohaem precursor [5], which has now been observed in sulfate-reducing bacteria and methanogenic archaea [6–8]. More recently, a third coproporphyrin-dependent pathway has been identified in Gram-positive bacteria [9,10] whereby coproporphyrinogen III is converted into protohaem via coproporphyrin III and Fe-coproporphyrin III intermediates. This pathway (Figure 1, blue route) has been reported to be more widely distributed and older than the classical protoporphyrin IX pathway (Figure 1, red route), pre-dating oxygenic photosynthesis [9]. It has long been known that certain Gram-positive bacteria, such as *Staphylococcus aureus*, accumulate coproporphyrin III and not protoporphyrin IX [11]. Interestingly, the enzyme HemY from *Bacillus subtilis* has been shown to oxidise both coproporphyrinogen III and protoporphyrinogen IX [12,13]. Further studies reported that a haem-binding protein HemQ that is required for the terminal steps of haem synthesis in species of Actinobacteria and Firmicutes had peroxidase and catalase activity and could stimulate the oxidation of protoporphyrin IX by HemY [14]. *S. aureus hemQ* mutants were then shown to accumulate coproporphyrin III, and the HemQ enzyme was reported to lyse haem in the presence of peroxide/chlorite [15]. Structural analyses then confirmed the HemQ family of proteins to be distinct from the original assignment to the family of chlorite dismutase enzymes [16]; these differences were defined by variations in conserved proximal/distal pocket residues [17]. However, an overlay of chlorite dismutase coordinates with the crystal structure of apo-HemQ from *Listeria monocytogenes* revealed the chlorite dismutase haem docks neatly in the HemQ active site cleft [18]. The true *in vivo* role for HemQ was revealed in 2015 when HemQ was confirmed to catalyse the decarboxylation of coprohaem for the non-canonical coproporphyrin-dependent pathway [9,10]. *Bona fide* coproporphyrinogen oxidases were shown to be absent from Actinobacteria and Firmicutes, explaining the lack of protoporphyrin IX in these organisms observed over four decades earlier [11]. The lack of a functional coproporphyrinogen oxidase in *S. aureus* was then validated by the report of a lack of activity for the purified HemN protein [10], which appears to have been misannotated [9]. Finally, the HemQ reaction was later shown to proceed via an unusual peroxide-dependent reaction via a harderohaem III intermediate [19], and FMN has also been shown to be an effective electron acceptor [9].

The current study seeks to investigate mechanisms that have driven the evolution of the classical protoporphyrin IX-dependent pathway present in proteobacteria and eukaryotes.

Since the HemQ component of the coproprophyrin pathway has been identified in evolutionarily early-branching (Acidobacteria and Planctomycetes) and transitional (*Deinococcus–Thermus* group) diderm phyla [9,20,21], it is highly likely that this pathway is an evolutionary precursor to the classical protoporphyrin IX pathway. However, the presence of a non-functional HemN homologue in the vast majority of Firmicutes/Actinobacteria [9], the identification of *hemF* genes in a small proportion of these families [9], and demonstrations that Gram-positive HemY enzymes can oxidise both protoporphyrinogen IX and copropophyrinogen III [9,13,14] all suggest that ancestral species of Firmicutes/Actinobacteria may have once produced both coproporphyrin III and protoporphyrin IX intermediates. The reported lack of protoporphyrin IX in Actinobacteria and Firmicutes [11] indicates that HemQ cannot convert coproporphyrin III into protoporphyrin IX, which is consistent with the requirement for a metallated porphyrin to participate in the peroxide-dependent HemQ mechanism [19].

Hence, one plausible route for the protoporphyrin-dependent pathway to have evolved is: (i) the necessary appearance of HemN/HemF enzyme(s) that decarboxylate coproporphyrinogen III to protoporphyrinogen IX, (ii) emergence of HemY variants that can oxidise both coproporphyrinogen III and protoporphyrinogen IX, (iii) emergence of HemH ferrochelatases that can catalyse iron insertion into coproporphyrin III and protoporphyrin IX, and finally (iv) loss of Fe-coproporphyrin III decarboxylases (HemQ/AhbD). Since there is a requirement for haem (or a significant growth advantage to synthesising it) in most organisms that have a functional haem biosynthetic pathway, it is plausible that the protoporphyrin- and coproporphyrin-dependent pathways coexisted before the protoporphyrin-dependent pathway came to predominate in proteobacteria and eukaryotes. Following this branching event, major clades have some interesting characteristics: HemQ/AhbD enzymes are largely absent from proteobacterial species that oxidise protoporphyinogen via the classical

Biochemical Journal (2016) **473** 3997–4009
DOI: 10.1042/BCJ20160696

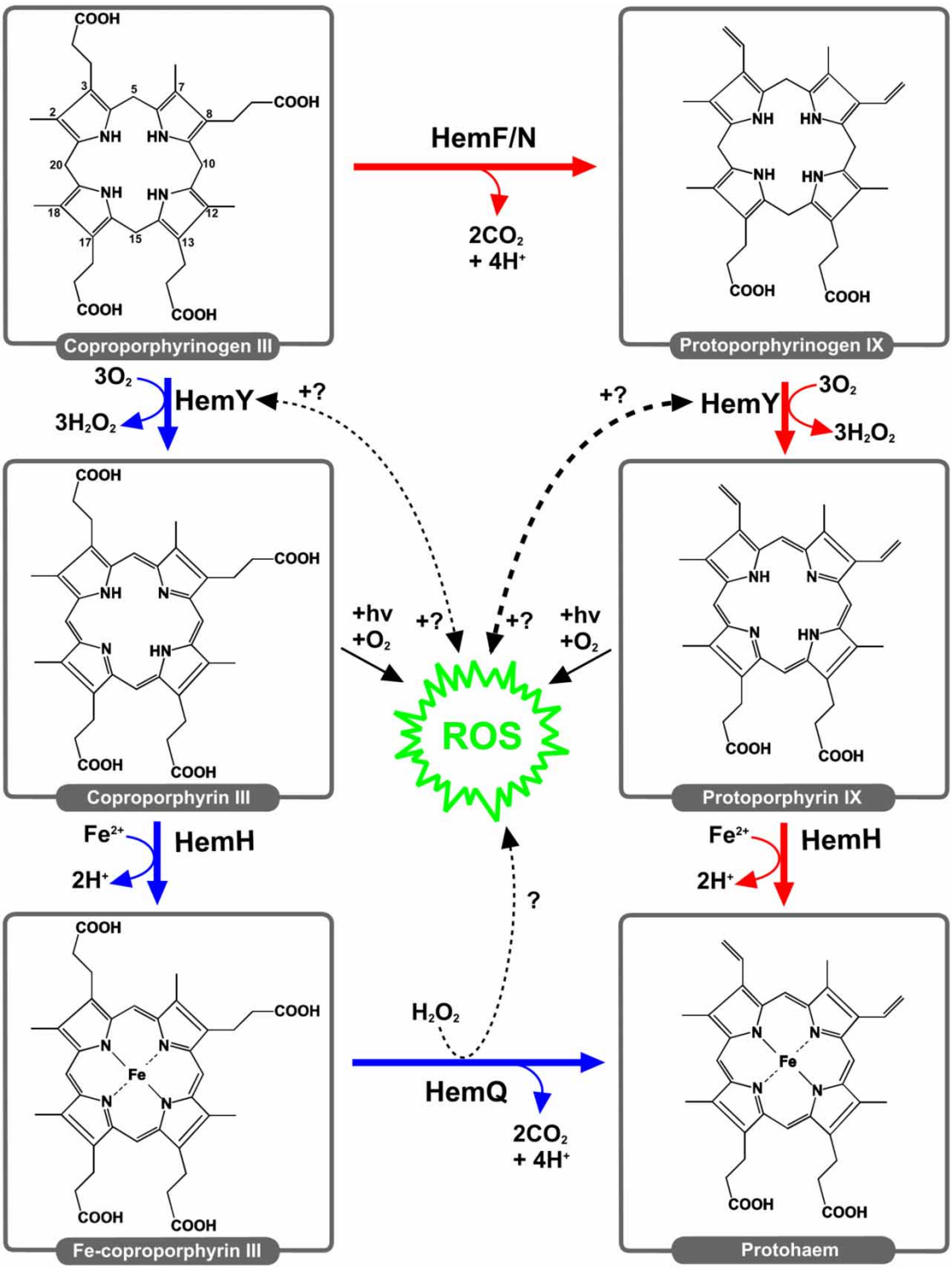

Figure 1. The classical and coproporphyrin-dependent pathways of haem synthesis.

This is a depiction of haem synthesis in a hypothetical ancestral organism in which the oxidation of coproporphyrinogen III to coproporphyrin III (blue) and the classical route, involving a protoporphyrin IX intermediate (red), takes place. HemQ is hypothesised to generate ROS, which, in turn, are hypothesised to have an impact on protoporphyrinogen IX oxidation to a greater extent than coproporphyrinogen III oxidation.

Biochemical Journal (2016) **473** 3997–4009
DOI: 10.1042/BCJ20160696

pathway, and Firmicutes/Actinobacteria possess HemQ/AhbD enzymes yet do not oxidise protoporphyrinogen IX to protoporphyrin IX. This exclusive presence of a classical or a coproprophyrin-dependent haem pathway is particularly intriguing in the light of demonstrations that HemQ stimulates protoporphyrinogen oxidation by *Propionibacterium acnes* HemY [14]. Since HemQ of *S. aureus* decarboxylates Fe-coproporphyrin III via a peroxide-dependent mechanism [19], it was hypothesised that radical generation by HemQ has a greater impact on protoporphyrinogen oxidation compared with coproporphyrinogen oxidation (Figure 1), resulting in the generation of reactive oxygen species (ROS) that are toxic to the cell. It was, therefore, of interest to re-evaluate substrate specificity in *S. aureus* HemY and to examine how the likely coexistence of HemY and HemQ influenced flux through the protoporphyrin IX (classical) and coproporphyrin III pathways. Here, we investigate this ancestral process in terms of how a combination of metalloporphyrin-bound HemQ and hydrogen peroxide influences the oxidation of porphyrinogen intermediates in both pathways (Figure 1).

Experimental

Protein purification

Recombinant *S. aureus* HemY and HemQ proteins were overexpressed and purified essentially as reported previously for other HemY proteins [22–25]. *Escherichia coli* BL21 pLysS cells were transformed with pET28a-*S. aureus hemY* [10] and pET14b-*S. aureus hemQ* [10], and starter cultures were grown overnight at 37°C and 160 rpm. Baffled flasks (2 litres) containing LB medium (1 litre) were inoculated and incubated at 37°C and 160 rpm until an OD_{600} of 0.6 had been reached, and 0.4 mM IPTG and 0.75 $\mu g \cdot ml^{-1}$ riboflavin were added at this point. Cultures were then grown for 16 h at 19°C and 160 rpm. Cells from 1 litre cultures were harvested by centrifugation and resuspended in a buffer (50 mM Tris/MOPS, pH 8.0, 100 mM KCl and 0.5% Tween 20) containing 1 $mg \cdot ml^{-1}$ phenylmethylsulfonyl fluoride, sonicated on ice for 6×30 s, and centrifuged at $100\,000 \times g$ (30 min) to remove membranes and insoluble proteins. The supernatant was applied to cobalt-chelate columns (2.5 ml bed volume) that were subsequently washed with 20 column volumes of a buffer and a further 20 volumes of buffer containing 15 mM imidazole. The purified proteins were eluted with a buffer containing 300 mM imidazole and concentrated to <1 ml. Imidazole was subsequently removed using PD10 desalting columns (GE Healthcare). Haem- and porphyrin-bound derivatives of HemY and HemQ were purified following the addition of tetrapyrroles prior to affinity chromatography, and the bound ligands were verified by absorption spectroscopy. Protein concentrations were determined spectrophotometrically using a Markwell assay [26].

Tetrapyrrole preparation

Protoporphyrin IX (3 mg) was solubilised with four drops of 30% ammonium hydroxide, and/or coproporphyrin III was solubilised with a few drops of DMSO. These porphyrins were then dissolved in 2.5 ml of freshly prepared 10 mM KOH containing 20% ethanol. This was then diluted with 2.5 ml of 10 mM KOH solution. Sodium amalgam was prepared, as previously described [27], by mixing 3.5 g of sodium metal with 75 g of mercury under a stream of nitrogen in a fume hood. The hot amalgam was cooled to room temperature, broken into 1 cm^3 pieces, and stored under nitrogen for up to 1 week. Immediately prior to use, 20 g of amalgam was pulverised with a mortar and pestle, and transferred to a flask under nitrogen in the dark. The 5 ml solution of porphyrin was transferred to the flask. The flask was sealed and shaken until the solution became colourless, making sure to vent any evolved gas. The pH was adjusted to 8.0 using a solution of 4 M MOPS. The resultant porphyrinogen solution (proto or copro) was filtered (using a 0.2 μm syringe filter), placed in the dark under nitrogen, and used immediately.

Haemin powder (Sigma) was solubilised in DMSO (Fluka) and was subsequently diluted in water. Protohaem IX solutions were quantified using a pyridine haemochrome assay [28] by mixing in a 1:1 ratio with a solution containing 4.2 M pyridine (Sigma) and 0.4 M NaOH. Reduced (sodium dithionite) minus oxidised (potassium ferricyanide) difference spectra were recorded, and haem concentrations were determined using a molar absorption coefficient of $\varepsilon_{557-541} = 20.7\ mM^{-1} \cdot cm^{-1}$ [29].

Assay of protoporphyrinogen oxidase and coproporphyrinogen oxidase activities

HemY activity was assayed using a continuous assay essentially as described previously [25].
This was performed on a FLUOstar OPTIMA plate reader using excitation and emission wavelengths of 520 and 620 nm, respectively.

Biochemical Journal (2016) **473** 3997–4009
DOI: 10.1042/BCJ20160696

The instrument was calibrated with known concentrations of protoporphyrin IX and coproporphyrin III. An opaque, clear-bottom, 96-well plate was used for the assays. The reaction mixtures were preincubated at 37°C in the dark for 3 min. The reactions were started by the addition of HemY (0.5 μM), which was also preincubated at 37°C, and the evolution of porphyrin was monitored for 30 min. The non-enzymatic rates were determined concomitantly and were subsequently subtracted. The total volume of the reaction mixture was 100 μl and contained 50 mM NaH_2PO_4, pH 8.0, and 0.2% Tween 20. The concentration of porphyrinogen substrate was determined retrospectively after the complete auto-oxidation of the stock solution to the porphyrin product, which was quantified spectrophotometrically. Molar absorption coefficients for protoporphyrin IX and coproprophyrin III were $\varepsilon_{408} = 262\ mM^{-1} \cdot cm^{-1}$ (in 2.7 M HCl) and $\varepsilon_{400} = 489\ mM^{-1} \cdot cm^{-1}$ (in 0.1 M HCl), respectively [30]. Horseradish peroxidase (HRP; 120–180 units/mg) and superoxide dismutase (SOD; ≥3000 units/mg) were obtained from Sigma and were included in the assays at concentrations indicated in the figure legends.

Structural modelling

Structural modelling was performed for HemQ enzymes using the RaptorX server at the University of Chicago [31,32]. Models for HemQ from *S. aureus* (SaHemQ) and *P. acnes* HemHQ residues 450–683 (PaHemQ) were generated using the crystal structure of HemQ from *Thermus thermophilus* (PDB code 1VDH [33]) as a template (α-carbon RMSD values for SaHemQ and PaHemQ were 0.34 and 0.75 Å, respectively). Structural modelling for HemQ from *Mycobacterium tuberculosis* (MtHemQ) was performed using the crystal structure of HemQ from *L. monocytogenes* (PDB code 4WWS [18]) as the most suitable template (α-carbon RMSD = 0.74 Å). To model a haem cofactor in the binding clefts, the α-carbon atoms of the closely related chlorite dismutase from *Candidatus* Nitrospira defluvii (PDB code 3NN1 [34]) were superimposed (RMSD values for SaHemQ, PaHemQ, and MtHemQ were 1.72, 1.51, and 1.68 Å, respectively).

Results

S. aureus HemY catalyses the oxidation of both protoporphyrinogen IX and coproporphyrinogen III

HemY enzymes from *B. subtilis* (a Firmicute), *P. acnes*, and *M. tuberculosis* (both Actinobacteria) have previously been shown to catalyse the oxidation of both protoporphyrinogen IX and coproporphyrinogen III

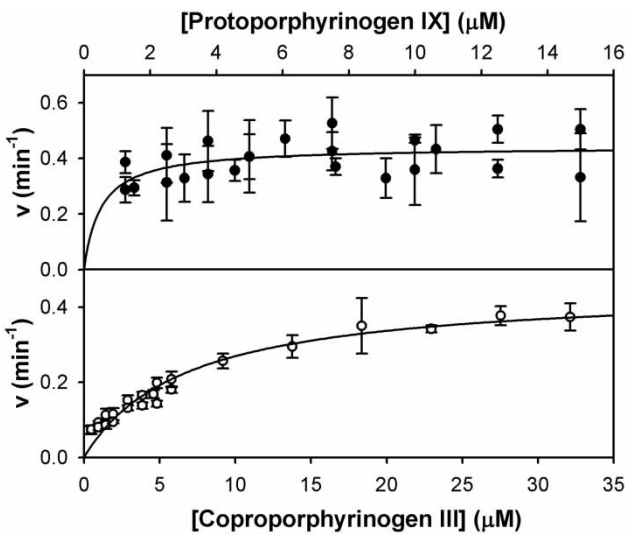

Figure 2. Kinetic analysis of the HemY protoporphyrinogen oxidase utilising protoporphyrinogen IX and coproporphyrinogen III substrates.

Non-linear regression analysis reveals k_{cat} values of 0.44 ± 0.03 and 0.46 ± 0.02 min^{-1} for protoporphyrinogen IX (●) and coproporphyrinogen III (○), respectively. The K_m for coproporphyrinogen III is 6.7 ± 0.8 μM.

Biochemical Journal (2016) **473** 3997–4009
DOI: 10.1042/BCJ20160696

[9,13,14], supporting the hypothesis that the classical haem pathway evolved from the coproporphyrin-dependent route. Hence, it was of interest to investigate whether the substrate specificity of HemY from *S. aureus* (a Firmicute) was consistent with these findings. Our kinetic analyses revealed k_{cat} values of 0.44 ± 0.03 and 0.46 ± 0.02 min^{-1} for protoporphyrinogen IX and coproporphyrinogen III, respectively (Figure 2). The K_m for coproporphyrinogen III was determined to be 6.7 ± 0.8 μM, whereas the K_m for protoporphyrinogen IX is likely to be lower than this but could not be accurately determined due to detection constraints at low substrate concentrations.

Haem-bound HemQ stimulates HemY-mediated oxidation of protoporphyrinogen but not coproporphyrinogen III

A major focus of the present study was to investigate why the classical pathway and coporphyrin-dependent pathways do not coexist. One hypothesis is that haem-bound HemQ produces toxic-free radicals in the presence of protoporphyrin IX and peroxide, whereas the less reactive coproporphyrin III product will not support this radical generation. There is a precedent for this, as the generation of superoxide by cytochrome *c* has previously been shown to stimulate the oxidation of protoporphyrinogen IX by a eukaryotic HemY enzyme [35]. We, therefore, aimed to test the hypothesis that any stimulation of HemY-catalysed protoporphyrinogen oxidation by haem-loaded HemQ, as observed previously for *P. acnes* HemY/HemQ [14], could be observed only when protoporphyrin IX is a reaction product (and not coproporphyrin III) and HemQ is specifically binding its haem product. Our data demonstrate that the presence of haem-loaded HemQ increased the k_{cat} for protoporphyrinogen oxidation by 2.6-fold (Figure 3), whereas the same experiment when coproporphyrinogen III was used as a substrate yielded no significant increase in activity in the presence of HemQ. To support the hypothesis that peroxidase-type chemistry of HemQ was contributing to this rate stimulation, HemY was assayed in the presence of HemQ that was loaded with bound haem, protoporphyrin IX, and coproporphyrin III (Figure 4). These data demonstrate that only haem-bound HemQ stimulates the HemY reaction, suggesting the involvement of peroxidase-like chemistry in this rate stimulation.

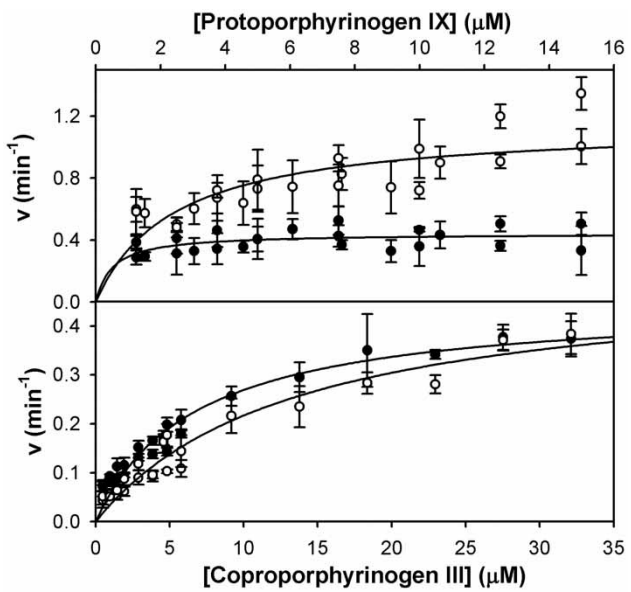

Figure 3. Haem-loaded HemQ stimulates HemY-mediated oxidation of protoporphyrinogen but not coproporphyrinogen III.

Steady-state kinetics for HemY in the presence (○) and absence (●) of haem-loaded HemQ (1 μM), using protoporphyrinogen IX (top panel) and coproporphyrinogen III (bottom panel) substrates. Non-linear regression analysis reveals a HemQ-mediated 2.6-fold increase in k_{cat} when protoporphyrinogen IX is used as a substrate, and a HemQ-mediated 1.1-fold increase in k_{cat} when coproporphyrinogen III is used as a substrate.

Biochemical Journal (2016) **473** 3997–4009
DOI: 10.1042/BCJ20160696

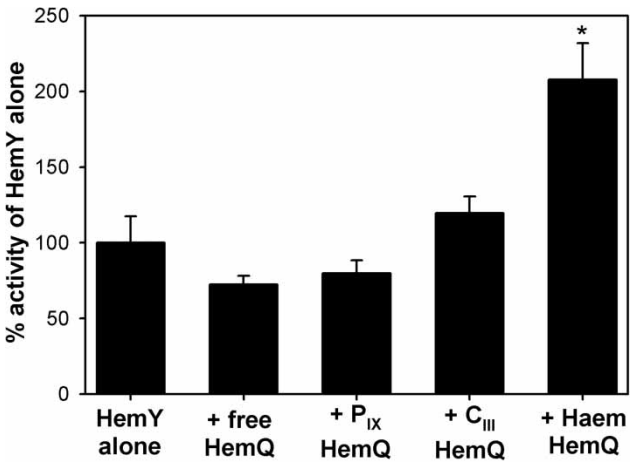

Figure 4. HemQ must bind haem for the stimulation of protoporphyrinogen oxidase activity.
Protoporphyrinogen oxidase activity of HemY was assayed in the presence of HemQ (1 μM) and protoporphyrinogen IX (10 μM) with different tetrapyrroles bound. Error bars represent SD values. Asterisk indicates that rates measured are significantly different from those measured using HemY alone (Student's *t*-test, $P < 0.05$).

Hydrogen peroxide participates in the HemQ-mediated stimulation of protoporphyrinogen IX oxidation via the generation of superoxide

We hypothesised that hydrogen peroxide produced during HemY catalysis was participating in the HemQ-mediated rate stimulation. To confirm the involvement of hydrogen peroxide, HemY-catalysed protoporphyrinogen IX oxidation was assayed in the presence and absence of haem-loaded HemQ at various concentrations of peroxide (Figure 5A). In the absence of HemQ, peroxide elicited a gradual decrease in activity, whereas, in the presence of HemQ, the peroxide caused a significant stimulation of protoporphyrinogen IX oxidation. The same experiment was performed with coproporphyrinogen III as a substrate, and peroxide did not elicit any changes in HemY catalysis in the presence or absence of HemQ (Figure 5B). To test the hypothesis that peroxidase chemistry was involved in the HemQ-mediated stimulation of HemY, protoporphyrinogen IX oxidation was measured in the presence of HRP (Figure 6), which demonstrated the same pattern of rate stimulation as haem-loaded HemQ (i.e. only when protoporphyrinogen IX was used as a substrate). To confirm that superoxide generation was involved in the HemQ-mediated stimulation of HemY, protoporphyrinogen IX oxidation was measured in the presence of superoxide dismutase (Figure 6), which completely abrogated the stimulatory effect of HRP. Since exogenous peroxide caused some inhibition of HemY in the absence of HemQ (Figure 5A), it was necessary to verify that the HRP stimulatory affect was not due to the *removal* of peroxide. The presence of catalase in HemY assays did not elicit a stimulatory effect (Figure 6), confirming that peroxide removal was not responsible for the stimulation of HemY-catalysed protoporphyrinogen IX oxidation.

HemQ enzymes possess a haem environment that is distinct from classical peroxidases

HemQ enzymes have recently been reported to lack a hydrogen-bonding network in the proximal haem-binding pocket that is present in closely related chlorite dismutase enzymes [17,18]. Such features are common in peroxidase-like enzymes that induce imidazolate character upon the axial histidine ligand that is important in catalysing the O–O bond cleavage reaction of haem-bound peroxides via the well-known 'push–pull' model [36] (to stabilise higher oxidation states of the haem iron during the peroxidase catalytic cycle). Since HemQ has recently been reported to proceed via a peroxide-dependent reaction [19] and the current data support the generation of superoxide by HemQ, it was of interest to revisit the structural components of the haem-binding cleft. Furthermore, previous structural analyses on HemQ-type enzymes have overlooked the members of this family that have been kinetically characterised and verified to be *bona fide* HemQ enzymes [17]. Hence, structural models for HemQ enzymes from *S. aureus*, *P. acnes*, and *M. tuberculosis* were generated using the

Biochemical Journal (2016) **473** 3997–4009
DOI: 10.1042/BCJ20160696

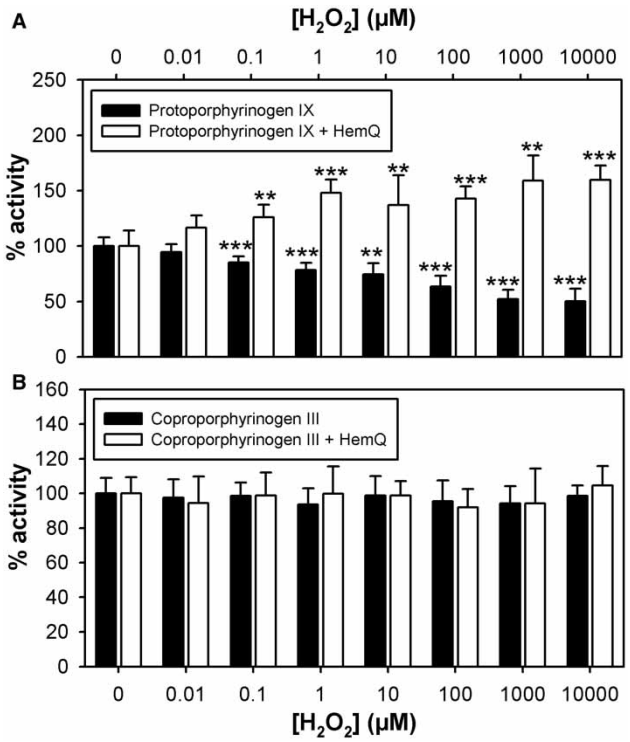

Figure 5. Hydrogen peroxide stimulates protoporphyrinogen oxidase activity in the presence of HemQ.
Protoporphyrinogen oxidase activity of HemY was assayed in the presence (1 μM) and absence of HemQ at various concentrations of hydrogen peroxide using 9.5 μM protoporphyrinogen IX (**A**) and 5.8 μM coproporphyrinogen III (**B**) as substrates. Error bars represent SD values. Asterisks indicate that rates measured are significantly different from those measured in the absence of peroxide (Student's *t*-test, $^{*}P < 0.05$, $^{**}P < 0.01$, $^{***}P < 0.001$).

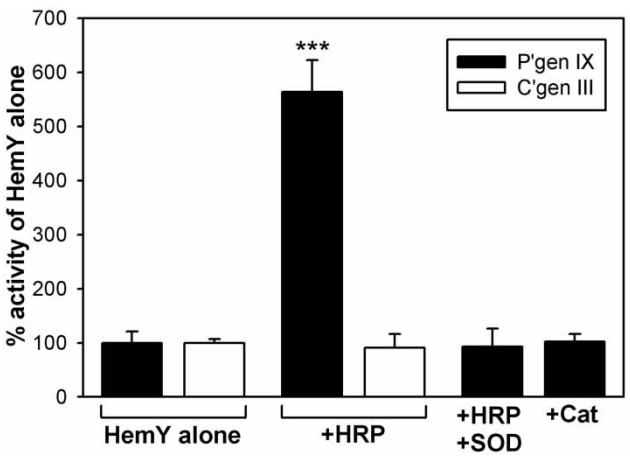

Figure 6. Peroxidase-derived superoxide stimulates HemY-mediated oxidation of protoporphyrinogen IX.
Kinetic assays showing the effect of HRP (1 μM), superoxide dismutase (1 μM), and catalase (1 μM) upon the activity of HemY (0.5 μM) using protoporphyrinogen IX (8.6 μM) and coproporphyrinogen III (8.2 μM) substrates. Abbreviations: HRP, horseradish peroxidase; SOD, superoxide dismutase; Cat, catalase; P'gen IX, protoporphyrinogen IX; C'gen III, coproporphyrinogen III. Asterisks indicate that rates measured are significantly different from those measured in the absence of peroxide (Student's *t*-test, $^{***}P < 0.001$).

Biochemical Journal (2016) **473** 3997–4009
DOI: 10.1042/BCJ20160696

RaptorX server [31,32], and the haem cofactor from the closely related chlorite dismutase from *Candidatus* Nitrospira defluvii (PDB code 3NN1 [34], Figure 7H) was overlaid (Figure 7A–C). Similarly, apoprotein crystal structures for enzymes that have been assigned to the HemQ family [16] were overlaid with the haem cofactor from 3NN1. These include 1VDH from *T. thermophilus* [33], 1T0T from *Bacillus stearothermophilus*, 4WWS from *L. monocytogenes* [18], and 3DTZ from *Thermoplasma acidophilum* (Figure 7D–G).

Initial comparisons of the distal pockets confirm that HemQ enzymes lack the conserved arginine that is common to chlorite dismutases (e.g. R173 in 3NN1): this position is labelled in red in Figure 7A–H and is most commonly occupied by a glutamine residue (e.g. Q185 in *S. aureus* HemQ), although this side chain is not necessary for the decarboxylation of Fe-coproporphyrin III as evidenced by alanine residues in this position for HemQ models for *P. acnes* and *M. tuberculosis* (Figure 7B,C). A multiple sequence alignment (Figure 7I) highlights a conserved tyrosine (Y145 in *S. aureus* HemQ) at the periphery of the distal cleft of HemQ enzymes (labelled in blue in Figure 7A–H), and an adjacent proline that is also fully conserved (P146 in *S. aureus* HemQ). Another notable observation is a conserved tryptophan residue adjacent to the haem

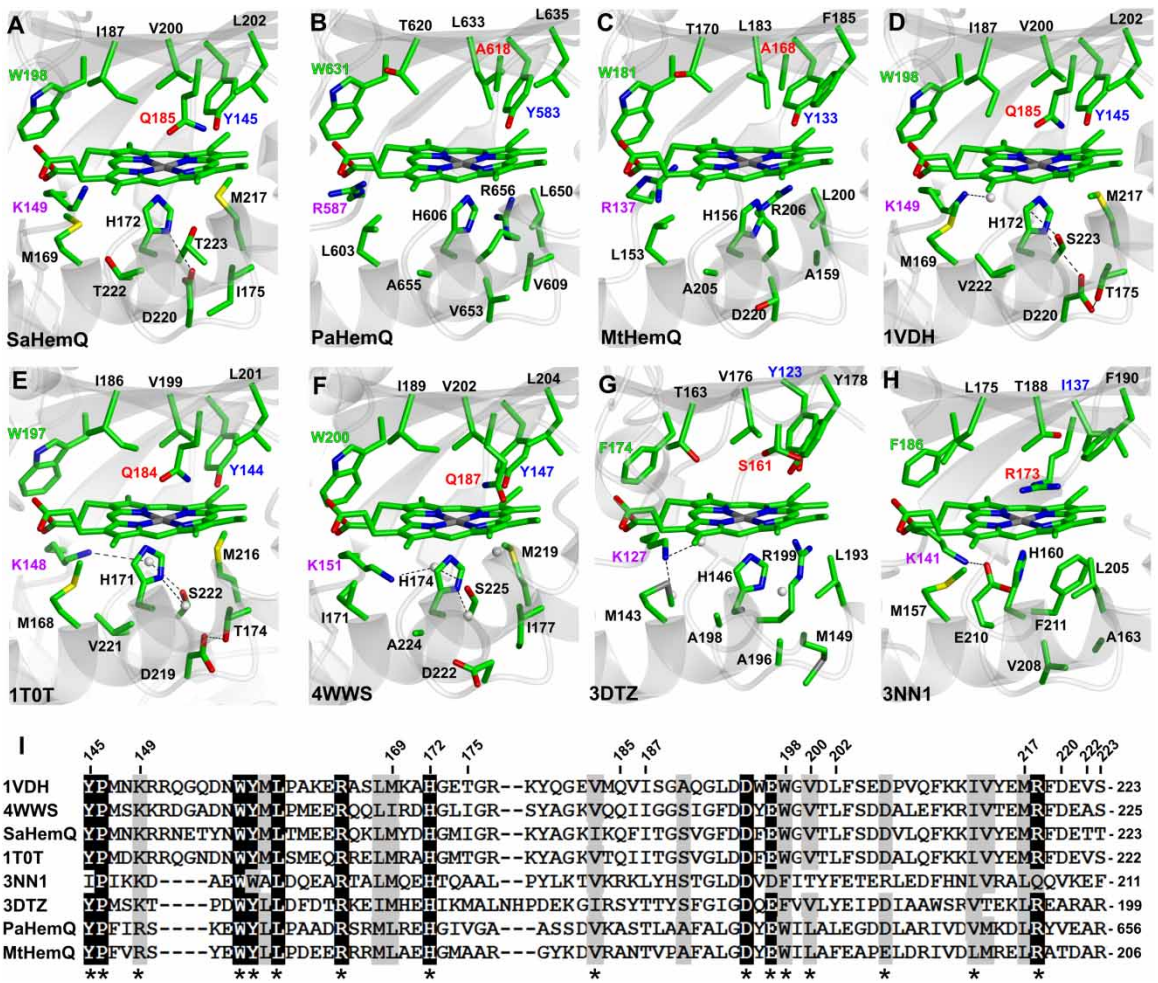

Figure 7. Structral analysis of the haem-binding cleft of HemQ family members.

Structural models of haem-binding clefts for HemQ enzymes from *S. aureus* (**A**, SaHemQ), *P. acnes* (**B**, PaHemQ), and *M. tuberculosis* (**C**, MtHemQ) were produced using the haem cofactor from the chlorite dismutase from *Candidatus* Nitrospira defluvii (**H**, 3NN1 [34]). (**D**–**G**) Apoprotein crystal structures of HemQ enzymes from *T. thermophilus* (1VDH [33]), *B. stearothermophilus* (1T0T), *L. monocytogenes* (4WWS [18]), and *T. acidophilum* (3DTZ), all with the haem cofactor from 3NN1 superimposed. (**I**) Multiple sequence alignment of sections of the proteins described above with residue numbers for SaHemQ marked at the top and functionally conserved residues marked with an asterisk.

Biochemical Journal (2016) **473** 3997–4009
DOI: 10.1042/BCJ20160696

propionates in Figure 7 (labelled in green in Figure 7A–H), although this residue is a phenylalanine in 3DTZ. There are no fully conserved residues in close proximity to the ubiquitous axial histidine in the proximal pocket for HemQ family members, although a lysine/arginine residue is present (K149 in *S. aureus* HemQ, labelled in purple in Figure 7A–H) that could potentially stabilise haem propionates or contribute to a proximal hydrogen-bonding network as in 3NN1 (albeit via water molecules). To gain greater insights into side chain requirements in and around the haem-binding cleft, residues that are fully or functionally conserved in the HemQ family were identified (asterisks on Figure 7I) and displayed on the model of *S. aureus* HemQ (Figure 8). This analysis revealed fully conserved tryptophan/tyrosine pair buried deep in the cleft (Figure 8, W157/Y158) and fully conserved arginine residues at opposite ends of the distal pocket (Figure 8, R165/R218). In addition, a fully conserved glutamate residue is adjacent to the conserved tryptophan (Figure 8, E197/W198) in the distal cleft. These observations provide insights into the required machinery for HemQ-mediated decarboxylation of Fe-coproprophyrin III and also have implications for the ability of HemQ enzymes to generate radicals that participate in the oxidation of porphyrinogen intermediates.

Discussion

This work examines the hypotheses that *S. aureus* HemY can participate in both the coproporphyrin-dependent and classical pathways, and that the generation of ROS by the HemQ enzyme has a more profound effect upon macrocycle oxidation in the classical pathway compared with the coproporphyrin-dependent pathway. These investigations will aid our understanding of how the classical pathway evolved from the more ancient coproporphyrin-dependent pathway [9].

Kinetic analysis of *S. aureus* HemY (Figure 2) revealed k_{cat} and K_m values of $0.46 \pm 0.02\ min^{-1}$ and $6.7 \pm 0.8\ \mu M$ for coproporphyrinogen III oxidation compared with previous measurements of $1.33 \pm 0.04\ min^{-1}$ and $0.31 \pm 0.01\ \mu M$ [10], respectively. Previously, the oxidation of protoporphyrinogen IX for *S. aureus* HemY could not be detected [10], so this reaction was re-examined. The data here clearly show activity for the protoporphyrinogen IX substrate ($k_{cat} = 0.44 \pm 0.03\ min^{-1}$), although the background rate and signal/noise ratio were significantly higher for the protoporphyrinogen IX reaction (Supplementary Figure S1), possibly explaining why enzymatic activity could not be detected in a recent study [10]. This pattern of substrate specificity is consistent with previous observations for HemY enzymes from numerous Actinobacteria/Firmicutes [9,13,14], and supports the hypothesis that evolutionary precursors of these HemY enzymes may once have also oxidised protoporphyrinogen IX *in vivo* in ancestral organisms. This is also supported by previous observations that the HemH ferrochelatases from Gram-positive bacteria can insert iron into both coproporphyrin III and protoporphyrin IX [9].

If we accept the compelling evidence that the classical pathway evolved from the coproporphyrin-dependent pathway, an important question presents itself: why do the majority of Actinobacteria/Firmicutes now lack a functional coproporphyrinogen oxidase that prevents the formation of protoporphyrinogen IX and protoporphyrin IX? One potential explanation would be that the peroxide-dependent mechanism of HemQ can generate free radicals, which will have a greater cytotoxic effect in combination with protoporphyrin IX compared with the less reactive coproporphyrin III. This is consistent with a previous report that the more reactive protoporphyrin IX causes greater cellular damage [37]. Hence, it was hypothesised that stimulation of HemY-mediated protoporphyrinogen IX oxidation by HemQ [14] was due to the evolution of ROS, as previously reported for cytochrome *c* and eukaryotic HemY [35], and that this stimulation would be exacerbated when protoporphyrin IX is a reaction product (compared with the less reactive coproporphyrin III). HemY assays with both substrates in the presence and absence of HemQ were consistent with this hypothesis (Figure 3), and yielded the surprising observation that HemQ did not stimulate the oxidation of coproporphyrinogen III at all. Further kinetic analysis with haem/porphyrin-loaded ligands confirms that haem, the product of the HemQ reaction, must be present for the stimulation of HemY activity (Figure 4). Further assays with various hydrogen peroxide concentrations (Figure 5) demonstrate that this ROS generator stimulates the HemY reaction only when HemQ is present, but causes inhibition in the absence of HemQ. Since the addition of high concentrations of peroxide resulted in a negligible stimulation in non-enzymatic oxidation of porphyrinogen substrate (Supplementary Figure S1), the most simple explanation for the inhibition of HemY by peroxide in the absence of HemQ is due to classical product inhibition. However, it is not clear why this does not take place when coproporphyrinogen III is used as a substrate (Figure 5B), although conformational differences in active site structure are likely to exist when additional propionates are present on the porphyrinogen substrate.

Biochemical Journal (2016) **473** 3997–4009
DOI: 10.1042/BCJ20160696

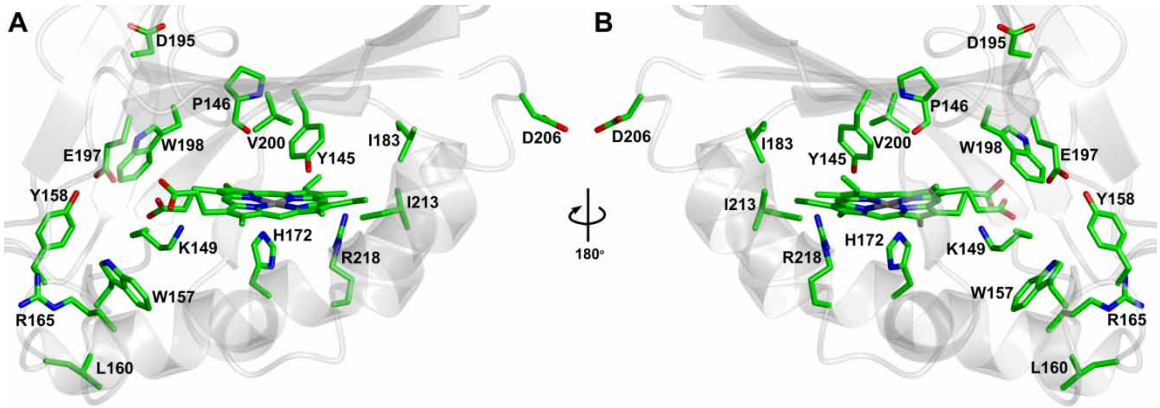

Figure 8. Conserved residues in the haem-binding cleft of HemQ family members.

Fully and functionally conserved residues in HemQ proteins from Figure 7I are represented on the structural model of *S. aureus* HemQ viewed from the entrance to the haem cleft (**A**) and from behind rotated 180° around the *y*-axis (**B**).

The stimulation of HemY activity by peroxide and HRP combined with the abrogation of this rate enhancement by SOD (Figure 6) provides clear confirmation that it is the peroxidase activity of HemQ that enhances HemY-mediated protoporphyrinogen IX oxidation. However, the previously reported rate constant for the peroxide-dependent evolution of protohaem of 1.6 min^{-1} is very low [16], which is consistent with a peroxidase-like active site for HemQ that lacks key features, such as a distal pocket arginine (that would stabilise a developing negative charge on the leaving group) and a proximal pocket hydrogen-bonding network (that would give the axial histidine imidazolate character to stabilise higher oxidation states of the iron during the peroxidase catalytic cycle). Previous structural analyses have focused on HemQ family members that lack biochemical confirmation as Fe-coproporphyrin III decarboxylases [17,18], so it was of interest to investigate HemQ enzymes from *S. aureus*, *P. acnes*, and *M. tuberculosis*, which have all been experimentally validated as HemQ enzymes. The structural modelling studies here (Figure 7) suggest that imidazolate character on the axial histidine is not necessary for catalysis, although some HemQ enzymes do possess hydrogen-bonding residues that could potentially polarise this residue. This is the case for *S. aureus* HemQ (Figure 7A), although previous resonance Raman data report a $\upsilon_{Fe\text{-}His}$ stretching mode of 213 cm^{-1} [16], which is consistent with a neutral axial ligand, although it is not clear whether haem or Fe-coproprophyrin III was bound in this study. Furthermore, while the majority of HemQ enzymes do possess a glutamine residue in place of the conserved distal arginine found in classical peroxidases, which could stabilise a positively charged leaving group, this residue is not necessary for HemQ activity as evidenced by alanine residues in this position for HemQ enzymes from *P. acnes* and *M. tuberculosis* (Figure 7B,C). Another notable absence in HemQ enzymes is a distal histidine residue, which, in classical peroxidases, acts as a base towards H_2O_2, catalysing the formation of the initial Fe^{III}-OOH (compound 0) intermediate [38]. In peroxidase mutants lacking an active site base, formation of compound 0 can be slowed by up to five orders of magnitude [39,40]. Furthermore, HemQ enzymes lack a conserved tryptophan residue that is found adjacent to the proximal histidine in classical peroxidases, which is the site of radical formation in compound I ([Fe(IV)═O Trp (·+)]). While peroxidases that lack such a proximal aromatic residue are likely to proceed via a porphyrin π-cation radical mechanism, the fully conserved distal tryptophan and tyrosine residues in HemQ enzymes (Figures 7I and 8 — Y145 and W198) are candidates for participation in radical-mediated decarboxylation of Fe-coprohaem. While the conserved doublet of W157/Y158 would provide a convenient tool for the decarboxylation of two propionate groups, a significant conformational change would be necessary to bring them into close proximity to the target β-carbon atoms. Together, these analyses are consistent with a HemQ enzyme that has evolved to have slow peroxidase activity (1.6 min^{-1} [16]), which fits well with measurements of the preceding ferrochelatase step (1.8 min^{-1} for *M. tuberculosis* HemH [9]).

Returning to the model in Figure 1, the current data are consistent with ROS generation by HemQ stimulating the HemY-catalysed oxidation of protoporphyrinogen IX only (and not stimulating the HemY-mediated oxidation of coproporphyrinogen III). However, one should not overlook the profound effect that HemQ has on the non-enzymatic oxidation of protoporphyrinogen IX (Supplementary Figure S1). While HemQ does appear to also elevate the non-enzymatic oxidation of coproporphyrinogen III, the overall rates are an order of

Biochemical Journal (2016) **473** 3997–4009
DOI: 10.1042/BCJ20160696

magnitude lower than those for protoporphyrinogen IX that are comparable with the HemY-catalysed turnover rates in Figure 2. This additional non-enzymatic rate enhancement is very likely to involve superoxide (from HemQ and possibly porphyrin-derived), adding weight to the hypothesis that peroxidase activity by HemQ will enhance the production of ROS in combination with tetrapyrrole intermediates of the classical pathway. Indeed, this mechanism is supported by our observations that reduced glutathione, a superoxide scavenger and common component of HemY assays, abolishes the stimulation of HemY-mediated protoporphyrinogen oxidation: this is why reduced glutathione is not present in the assays described here. From an evolutionary perspective, this generation of toxic ROS would provide a selection pressure to retain either the coproporphyrin-dependent pathway *or* the classical pathway, but not both. This model is also consistent with observations that HemQ enzymes may utilise alternative electron acceptors such as FMN, negating the requirement for HemY-derived peroxide in the coproporphyrin-dependent pathway. This may also explain why in proteobacteria that commonly utilise the classical pathway, HemJ or HemG enzymes that do not require oxygen nor produce hydrogen peroxide are the most common forms of protoporphyrinogen oxidase [4,9].

Abbreviations

HRP, horseradish peroxidase; MtHemQ, HemQ from *Mycobacterium tuberculosis*; PaHemQ, HemHQ from *Propionibacterium acnes*; PPO, protoporphyrinogen IX oxidase; ROS, reactive oxygen species; SaHemQ, HemQ from *Staphylococcus aureus*; SOD, superoxide dismutase.

Author Contribution

C.H. performed the experiments and M.S. drove the experimental design. C.H. and M.S. analysed the data. C.H., H.A.D., and M.S. wrote the paper.

Funding

This work was funded by a Research Grant from the Royal Society [RG110528 to M.S.].

Acknowledgements

We thank the laboratories of Professor Martin Warren (University of Kent) and Professor Harry Dailey (University of Georgia) for supplying expression plasmids for HemY and HemQ.

Competing Interests

The Authors declare that there are no competing interests associated with the manuscript.

References

1 Layer, G., Reichelt, J., Jahn, D. and Heinz, D.W. (2010) Structure and function of enzymes in heme biosynthesis. *Prot. Sci.* **19**, 1137–1161 doi:10.1002/pro.405
2 Mobius, K., Arias-Cartin, R., Breckau, D., Hannig, A.-L., Riedmann, K., Biedendieck, R. et al. (2010) Heme biosynthesis is coupled to electron transport chains for energy generation. *Proc. Natl Acad. Sci. USA* **107**, 10436–10441 doi:10.1073/pnas.1000956107
3 Jacobs, N.J. and Jacobs, J.M. (1976) Nitrate, fumarate, and oxygen as electron acceptors for a late step in microbial heme synthesis. *Biochim. Biophys. Acta Bioenergetics* **449**, 1–9 doi:10.1016/0005-2728(76)90002-5
4 Kobayashi, K., Masuda, T., Tajima, N., Wada, H. and Sato, N. (2014) Molecular phylogeny and intricate evolutionary history of the three isofunctional enzymes involved in the oxidation of protoporphyrinogen IX. *Genome Biol. Evol.* **6**, 2141–2155 doi:10.1093/gbe/evu170
5 Buchenau, B., Kahnt, J., Heinemann, I.U., Jahn, D. and Thauer, R.K. (2006) Heme biosynthesis in *Methanosarcina barkeri* via a pathway involving two methylation reactions. *J. Bacteriol.* **188**, 8666–8668 doi:10.1128/JB.01349-06
6 Palmer, D.J., Schroeder, S., Lawrence, A.D., Deery, E., Lobo, S.A., Saraiva, L.M. et al. (2014) The structure, function and properties of sirohaem decarboxylase — an enzyme with structural homology to a transcription factor family that is part of the alternative haem biosynthesis pathway. *Mol. Microbiol.* **93**, 247–261 doi:10.1111/mmi.12656
7 Lobo, S.A.L., Lawrence, A.D., Romao, C.V., Warren, M.J., Teixeira, M. and Saraiva, L.M. (2014) Characterisation of *Desulfovibrio vulgaris* haem *b* synthase, a radical SAM family member. *Biochim. Biophys. Acta Proteins Proteom.* **1844**, 1238–1247 doi:10.1016/j.bbapap.2014.03.016
8 Bali, S., Lawrence, A.D., Lobo, S.A., Saraiva, L.M., Golding, B.T., Palmer, D.J. et al. (2011) Molecular hijacking of siroheme for the synthesis of heme and d_1 heme. *Proc. Natl Acad. Sci. USA* **108**, 18260–18265 doi:10.1073/pnas.1108228108
9 Dailey, H.A., Gerdes, S., Dailey, T.A., Burch, J.S. and Phillips, J.D. (2015) Noncanonical coproporphyrin-dependent bacterial heme biosynthesis pathway that does not use protoporphyrin. *Proc. Natl Acad. Sci. USA* **112**, 2210–2215 doi:10.1073/pnas.1416285112
10 Lobo, S.A., Scott, A., Videira, M.A., Winpenny, D., Gardner, M., Palmer, M.J. et al. (2015) *Staphylococcus aureus* haem biosynthesis: characterisation of the enzymes involved in final steps of the pathway. *Mol. Microbiol.* **97**, 472–487 doi:10.1111/mmi.13041
11 Jacobs, N.J., Jacobs, J.M. and Brent, P. (1971) Characterization of the late steps of microbial heme synthesis: conversion of coproporphyrinogen to protoporphyrin. *J. Bacteriol.* **107**, 203–209 PMCID:246905
12 Dailey, T.A., Meissner, P. and Dailey, H.A. (1994) Expression of a cloned protoporphyrinogen oxidase. *J. Biol. Chem.* **269**, 813–815 PMID: 8288631

13 Hansson, M. and Hederstedt, L. (1994) *Bacillus subtilis* HemY is a peripheral membrane protein essential for protoheme IX synthesis which can oxidize coproporphyrinogen III and protoporphyrinogen IX. *J. Bacteriol.* **176**, 5962–5970 PMID:7928957
14 Dailey, T.A., Boynton, T.O., Albetel, A.-N., Gerdes, S., Johnson, M.K. and Dailey, H.A. (2010) Discovery and characterization of HemQ: an essential heme biosynthetic pathway component. *J. Biol. Chem.* **285**, 25978–25986 doi:10.1074/jbc.M110.142604
15 Mayfield, J.A., Hammer, N.D., Kurker, R.C., Chen, T.K., Ojha, S., Skaar, E.P. et al. (2013) The chlorite dismutase (HemQ) from *Staphylococcus aureus* has a redox-sensitive heme and is associated with the small colony variant phenotype. *J. Biol. Chem.* **288**, 23488–23504 doi:10.1074/jbc.M112.442335
16 Celis, A.I. and DuBois, J.L. (2015) Substrate, product, and cofactor: the extraordinarily flexible relationship between the CDE superfamily and heme. *Arch. Biochem. Biophys.* **574**, 3–17 doi:10.1016/j.abb.2015.03.004
17 Hofbauer, S., Howes, B.D., Flego, N., Pirker, K.F., Schaffner, I., Mlynek, G. et al. (2016) From chlorite dismutase towards HemQ — the role of the proximal H-bonding network in haeme binding. *Biosci. Rep.* **36**, e00312 doi:10.1042/BSR20150330
18 Hofbauer, S., Hagmüller, A., Schaffner, I., Mlynek, G., Krutzler, M., Stadlmayr, G. et al. (2015) Structure and heme-binding properties of HemQ (chlorite dismutase-like protein) from *Listeria monocytogenes*. *Arch. Biochem. Biophys.* **574**, 36–48 doi:10.1016/j.abb.2015.01.010
19 Celis, A.I., Streit, B.R., Moraski, G.C., Kant, R., Lash, T.D., Lukat-Rodgers, G.S. et al. (2015) Unusual peroxide-dependent, Heme-transforming reaction catalyzed by HemQ. *Biochemistry* **54**, 4022–4032 doi:10.1021/acs.biochem.5b00492
20 Gupta, R.S. (1998) Protein phylogenies and signature sequences: a reappraisal of evolutionary relationships among archaebacteria, eubacteria, and eukaryotes. *Microbiol. Mol. Biol. Rev.* **62**, 1435–1491 PMID:9841678
21 Gupta, R.S. (2011) Origin of diderm (Gram-negative) bacteria: antibiotic selection pressure rather than endosymbiosis likely led to the evolution of bacterial cells with two membranes. *Anton. Leeuw.* **100**, 171–182 doi:10.1007/s10482-011-9616-8
22 Dailey, T.A. and Dailey, H.A. (1996) Human protoporphyrinogen oxidase: expression, purification, and characterization of the cloned enzyme. *Prot. Sci.* **5**, 98–105 doi:10.1002/pro.5560050112
23 Dailey, H.A. and Dailey, T.A. (1996) Protoporphyrinogen oxidase of *Myxococcus xanthus*: expression, purification, and characterization of the cloned enzyme. *J. Biol. Chem.* **271**, 8714–8718 doi:10.1074/jbc.271.15.8714
24 Wang, K.-F., Dailey, T.A. and Dailey, H.A. (2001) Expression and characterization of the terminal heme synthetic enzymes from the hyperthermophile *Aquifex aeolicus*. *FEMS Microbiol. Lett.* **202**, 115–119 doi:10.1111/j.1574-6968.2001.tb10789.x
25 Shepherd, M. and Dailey, H.A. (2005) A continuous fluorimetric assay for protoporphyrinogen oxidase by monitoring porphyrin accumulation. *Anal. Biochem.* **344**, 115–121 doi:10.1016/j.ab.2005.06.012
26 Markwell, M.A.K., Haas, S.M., Bieber, L.L. and Tolbert, N.E. (1978) A modification of the Lowry procedure to simplify protein determination in membrane and lipoprotein samples. *Anal. Biochem.* **87**, 206–210 doi:10.1016/0003-2697(78)90586-9
27 Brenner, D.A. and Bloomer, J.R. (1980) A fluorometric assay for measurement of protoporphyrinogen oxidase activity in mammalian tissue. *Clin. Chim. Acta* **100**, 259–266 doi:10.1016/0009-8981(80)90275-2
28 Berry, E.A. and Trumpower, B.L. (1987) Simultaneous determination of hemes *a*, *b*, and *c* from pyridine hemochrome spectra. *Anal. Biochem.* **161**, 1–15 doi:10.1016/0003-2697(87)90643-9
29 Smith, K.M. (1975) *Porphyrins and Metalloporphyrins*, Elsevier, New York
30 Falk, J.E. (1964) *Porphyrins and Metalloporphyrins: Their General, Physical and Coordination Chemistry, and Laboratory Methods*, Elsevier, Amsterdam
31 Käellberg, M., Wang, H., Wang, S., Peng, J., Wang, Z., Lu, H. et al. (2012) Template-based protein structure modeling using the RaptorX web server. *Nat. Protoc.* **7**, 1511–1522 doi:10.1038/nprot.2012.085
32 Peng, J. and Xu, J. (2011) RaptorX: exploiting structure information for protein alignment by statistical inference. *Proteins Struct. Funct. Bioinformatics* **79**, 161–171 doi:10.1002/prot.23175
33 Ebihara, A., Okamoto, A., Kousumi, Y., Yamamoto, H., Masui, R., Ueyama, N. et al. (2005) Structure-based functional identification of a novel heme-binding protein from *Thermus thermophilus* HB8. *J. Struct. Funct. Genomics* **6**, 21–32 doi:10.1007/s10969-005-1103-x
34 Kostan, J., Sjöeblom, B., Maixner, F., Mlynek, G., Furtmüeller, P.G., Obinger, C. et al. (2010) Structural and functional characterisation of the chlorite dismutase from the nitrite-oxidizing bacterium '*Candidatus Nitrospira defluvii*': identification of a catalytically important amino acid residue. *J. Struct. Biol.* **172**, 331–342 doi:10.1016/j.jsb.2010.06.014
35 Shepherd, M. and Dailey, H.A. (2009) Peroxidase activity of cytochrome *c* facilitates the protoporphyrinogen oxidase reaction. *Cell Mol. Biol.* **55**, 6–14 PMID:19267995
36 Poulos, T.L. (1996) The role of the proximal ligand in heme enzymes. *J. Biol. Inorg. Chem.* **1**, 356–359 doi:10.1007/s007750050064
37 Aravind Menon, I., Persad, S.D. and Haberman, H.F. (1989) A comparison of the phototoxicity of protoporphyrin, coproporphyrin and uroporphyrin using a cellular system in vitro. *Clin. Biochem.* **22**, 197–200 doi:10.1016/S0009-9120(89)80077-3
38 Poulos, T.L. and Fenna, R.E. (1994) In *Metal Ions in Biololgical Systems* (Sigel, H. and Sigel, A., eds.), vol. 30, pp. 25–75, Dekker, New York
39 Hiner, A.N., Raven, E.L., Thorneley, R.N., García-Caìnovas, F. and Rodríguez-Loìpez, J.N. (2002) Mechanisms of compound I formation in heme peroxidases. *J. Inorg. Biochem.* **91**, 27–34 doi:10.1016/S0162-0134(02)00390-2
40 Erman, J.E., Vitello, L.B., Miller, M.A., Shaw, A., Brown, K.A. and Kraut, J. (1993) Histidine 52 is a critical residue for rapid formation of cytochrome *c* peroxidase compound I. *Biochemistry* **32**, 9798–9806 doi:10.1021/bi00088a035

